10574 *Biochemistry* **2010,** *49,* 10574–10581
DOI: 10.1021/bi101521p

BIOCHEMISTRY
including biophysical chemistry & molecular biology
Article

Consecutive Terminal GU Pairs Stabilize RNA Helices[†]

Mai-Thao Nguyen and Susan J. Schroeder*

Department of Chemistry and Biochemistry and Department of Botany and Microbiology, University of Oklahoma, 101 Stephenson Parkway, Norman, Oklahoma 73019, United States

Received September 18, 2010; Revised Manuscript Received November 8, 2010

ABSTRACT: Consecutive GU pairs at the ends of RNA helices provide significant thermodynamic stability between −1.0 and −3.8 kcal/mol at 37 °C, which is equivalent to approximately 2 orders of magnitude in the value of a binding constant. The thermodynamic stabilities of GU pairs depend on the sequence, stacking orientation, and position in the helix. In contrast to GU pairs in the middle of a helix that may be destabilizing, all consecutive terminal GU pairs contribute favorable thermodynamic stability. This work presents measured thermodynamic stabilities for 30 duplexes containing two, three, or four consecutive GU pairs at the ends of RNA helices and a model to predict the thermodynamic stabilities of terminal GU pairs. Imino proton NMR spectra show that the terminal GU nucleotides form hydrogen-bonded pairs. Different orientations of terminal GU pairs can have different conformations with equivalent thermodynamic stabilities. These new data and prediction model will help improve RNA secondary structure prediction, identification of miRNA target sequences with GU pairs, and efforts to understand the fundamental physical forces directing RNA structure and energetics.

The power of RNA to regulate gene expression holds the promise of revolutionizing therapeutic approaches to disease and investigations of genomic biology (*1*, *2*). Realizing the full potential of RNA silencing requires knowledge of the fundamental physical forces that stabilize RNA duplex formation. The efficacy of small RNA binding to mRNA target sites correlates with the stability of miRNA−mRNA duplexes and can be predicted by using thermodynamic parameters of RNA motifs and computer algorithms (*3*−*7*). An exception to this observation occurs with the idiosyncratic GU base pair, the thermodynamic stability of which is poorly predicted. Even a single GU base pair added to the 5′ region of the miRNA can decrease silencing activity (*4*). For example, in luciferase assays in HeLa cells, changing a single GC pair to a GU pair abolished translational repression by endogenous let-7 (*4*). Similarly, changing an AU pair to a GU pair reduced the level of translational repression by CXCR4 siRNA from 12- to 6-fold even though the predicted free energies of the miRNA−mRNA duplexes were the same (*4*). Therefore, improved thermodynamic parameters for GU base pairs are necessary for improving predictions of siRNA target sites and designing new therapeutics.

Previous studies of the thermodynamic stabilities of consecutive terminal mismatches and dangling ends demonstrate significant improvement in the prediction of duplex stabilities with new parameters that included the additional stabilities of up to three nucleotides stacking on the 3′ end of a helix (*8*). The sequence identity of the 5′ nucleotides does not contribute significant additional thermodynamic stability, but GU pairs are the exception to this observation. Previous studies of single GU pairs at the ends of helices (*9*) show favorable thermodynamic stabilities, while duplexes with single internal GU pairs are unfavorable relative to duplexes with equivalent Watson−Crick pairs (*10*). Tandem internal GU pairs are energetically unfavorable (from 0.3 to 1.3 kcal/mol) with one context-dependent exception in the case of 5′GGUC/3′CUGG (−1.1 kcal/mol) (*11*−*14*). GU pairs adjacent to internal loops show idiosyncratic stabilities (*15*−*17*). The physical basis of these idiosyncratic thermodynamic stabilities may be the ability of GU pairs to adopt many different stable hydrogen-bonded conformations. GU pairs can form with either one or two hydrogen bonds in many different orientations; four representative examples from the isostericity matrices of Leontis and Westof are shown in Figure 1 (*14*, *18*). The thermodynamic stabilities and structures of GU pairs show idiosyncratic, sequence-dependent, non-nearest-neighbor effects.

To gain further insight into non-nearest-neighbor effects and GU base pairs, terminal single, double, triple, and quadruple GU base pairs are analyzed using UV optical melting and one-dimensional proton NMR. All terminal GU motifs add stability to the duplexes and are more stable than predicted. Using thermodynamics data and linear regression, a new model was developed for predicting the stabilities of terminal GU base pairs.

METHODS

Oligoribonucleotides were purchased from Dharmacon and deblocked with acetic acid to remove the protection group on its 2′-hydroxyl as per the manufacturer's instructions. Greater than 90% oligomer purity was confirmed using ^{32}P labeling and gel electrophoresis.

Oligonucleotides were resuspended in 1 M NaCl, 10 mM sodium cacodylate, 0.5 mM Na_2EDTA (pH 7) melting buffer. As noted in Table 1, some oligonucleotides were also melted in 0.15 M KCl, 10 mM $MgCl_2$, 10 mM sodium cacodylate, 0.1 mM Na_2EDTA (pH 7) melting buffer. Ten different oligonucleotide concentrations over a 100-fold range were used in a Beckman

[†]This work was supported by Oklahoma Center for the Advancement of Science and Technology Grant HR09-160, an American Cancer Society Institutional Research Grant to the University of Oklahoma Cancer Center (Seed Grant 090039), and National Science Foundation Grant 0844913.

*To whom correspondence should be addressed. E-mail: susan.schroeder@ou.edu. Phone: (405) 325-3092. Fax: (405) 325-6111.

 Published on Web 11/10/2010

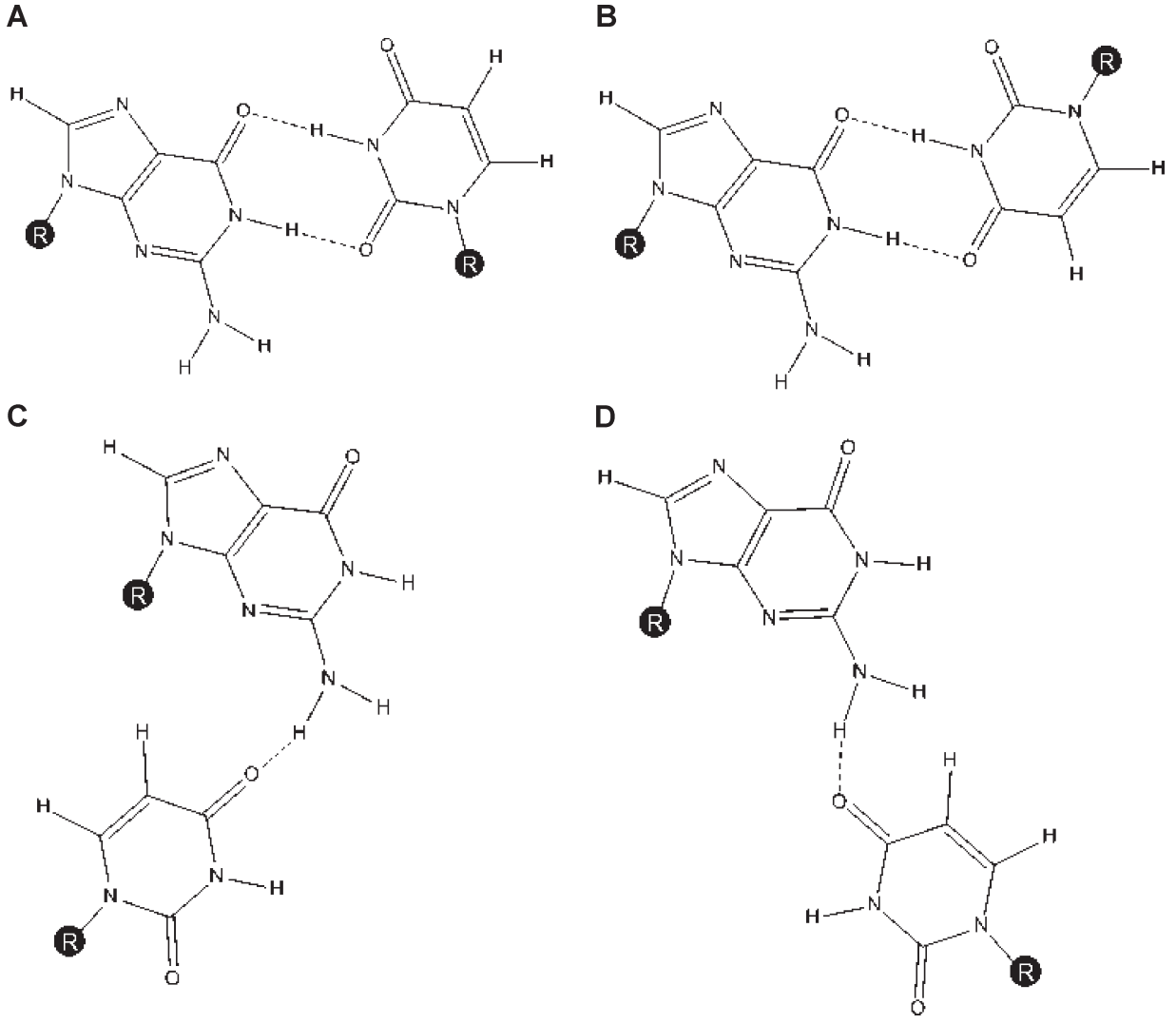

FIGURE 1: Examples of GU pair conformations with one or two hydrogen bonds (*18*): (A) cis Watson−Crick−Watson−Crick, (B) trans Watson−Crick−Watson−Crick, (C) cis Hoogsteen−sugar edge, and (D) trans Hoogsteen−sugar edge.

Coulter DU800 spectrophotometer at wavelengths of 280 and 260 nm with a heating rate of 1 °C/min. Melting curves were fit to a two-state model with Meltwin (*12*, *19*). The inverse of the melting temperature was plotted against the log of the total strand concentration according to the following equation:

$$\frac{1}{T_M} = \frac{R \ln(C_T)}{\Delta H^\circ} + \frac{\Delta S^\circ}{\Delta H^\circ} \quad (1)$$

where R is the gas constant (*20*). If the thermodynamic parameters for the duplexes derived from plots of T_M^{-1} versus $\ln(C_T)$ and from the average of curve fittings agree within 15%, then the results are consistent with the two-state transition model (*21*). The thermodynamic parameters listed in Table 1 are consistent with the two-state model.

Selected duplexes were analyzed by one-dimensional imino proton NMR using a 500 MHz Varian VNMR spectrometer. Oligomers were dissolved at 0.4 mM RNA in 10 mM NaCl, 10 mM sodium phosphate, 0.5 mM Na_2EDTA (pH 6), and 10% D_2O. The watergate 3414 pulse sequence in the Biopack software was used for water suppression (*22*).

Linear regression analysis was used to determine a model for predicting the thermodynamic stabilities of GU terminal motifs. Excel and the linest function were used for the analysis. Data from previous studies of single terminal GU pairs (*9*, *11*, *23*) and the new data in Table 1 are included in this regression. Statistical significance is determined from the T and P tests in Excel.

RESULTS

Table 1 presents 30 new thermodynamic measurements of RNA duplexes containing consecutive terminal GU pairs. The additional stability derived from the consecutive terminal GU pair motifs ranges from −1.0 to −3.8 kcal/mol at 37 °C; the 2.8 kcal/mol difference in free energies is approximately 2 orders of magnitude in a binding constant at 37 °C. The thermodynamic stabilities per nucleotide in consecutive terminal GU pair motifs range from −0.2 to −0.6 kcal/mol. The sequences are listed by number of GU pairs and then increasingly favorable free energy for the terminal pairs. All possible combinations of GU pair and neighboring Watson−Crick pair orientations have been measured for single and tandem terminal GU pairs. To compare duplexes with different core stem helices, we calculated the free energy of the terminal motif with the following equation:

$$\Delta\Delta G^\circ_{\text{terminal motif}} = (\Delta G^\circ_{\text{duplex with terminal motif}} - \Delta G^\circ_{\text{duplex without terminal motif}})/2 \quad (2)$$

All the duplexes with more than one GU pair are more favorable than previously predicted (*11*, *24*).

Table 1: Thermodynamic Parameters of RNA Duplexes with Terminal GU and AU Pairs[a]

				T_M^{-1} vs ln(C_T/A)				melt curve fits			
GU pair	sequence[b]	$-\Delta\Delta G°_{37}$[c] (kcal/mol)	$-\Delta G°_{37\text{predicted}}$[d] (kcal/mol)	$-\Delta G°_{37}$ (kcal/mol)	$-\Delta H°$ (kcal/mol)	$-\Delta S°$ (eu)	T_m[e] (°C)	$-\Delta G°_{37}$ (kcal/mol)	$-\Delta H°$ (kcal/mol)	$-\Delta S°$ (eu)	T_m[e] (°C)
1	5′**UUGCAG**[i]	1.0 ± 0.2	3.3 ± 0.1	4.2 ± 0.2	37.2 ± 3.8	106.5 ± 12.8	25.3	4.3 ± 0.3	35.5 ± 6.6	100.4 ± 22.2	25.7
1	5′**UAUGCAUG**[i]	1.0 ± 0.1	6.4 ± 0.1	6.4 ± 0.1	62.3 ± 3.1	180.1 ± 9.0	41.0	6.5 ± 1.3	57.7 ± 2.9	165.1 ± 8.3	41.4
1	5′**GAUGCAUU**[i]	1.2 ± 0.1	7.0 ± 0.1	6.8 ± 0.1	62.9 ± 3.1	180.8 ± 9.0	42.6	6.8 ± 1.4	60.8 ± 3.0	174.0 ± 8.7	42.9
1	5′**GUGCAU**[f,j]	1.4 ± 0.1	4.8 ± 0.1	5.1 ± 0.1	47.5 ± 2.4	136.9 ± 7.7	33.1	5.1 ± 0.1	47.0 ± 3.6	135.0 ± 11.5	33.4
1	5′**UCCGGG**[h]	1.5 ± 0.1	6.5 ± 0.1	7.4 ± 0.1	47.7 ± 2.4	129.8 ± 6.5	48.5	7.4 ± 1.5	47.4 ± 2.4	129.0 ± 6.5	48.6
1	5′**UGGCCG**[h]	1.6 ± 0.1	7.3 ± 0.1	8.6 ± 0.2	53.0 ± 2.7	143.3 ± 7.2	54.7	8.3 ± 1.7	49.8 ± 2.5	133.7 ± 6.7	54.9
1	5′**GGCGCU**[h]	1.9 ± 0.1	8.0 ± 0.1	8.4 ± 0.2	56.4 ± 2.8	154.7 ± 7.7	52.9	8.4 ± 1.7	55.9 ± 2.8	153.0 ± 7.7	53.0
1	5′**GCCGGU**[h]	2.4 ± 0.1	8.5 ± 0.1	9.2 ± 0.2	58.2 ± 2.9	158.1 ± 7.9	57.0	9.3 ± 1.9	59.3 ± 3.0	161.2 ± 8.1	57.0
2	5′**UUUGCAGG**	1.3 ± 0.2	3.2 ± 0.2	4.8 ± 0.2	46.1 ± 3.7	133.1 ± 12.3	31.1	5.0 ± 0.4	40.7 ± 6.1	115.2 ± 20.5	31.8
2	5′**UUAUCGAUGG**[f,j]	1.5 ± 0.1	4.9 ± 0.1	6.8 ± 0.1	61.1 ± 4.5	175.0 ± 14.4	43.2	6.9 ± 0.1	57.0 ± 7.0	161.5 ± 22.8	44.0
2	5′**GUUGCAGU**[g,l]	1.6 ± 0.2	5.8 ± 0.1	5.4 ± 0.1	45.2 ± 3.7	128.3 ± 12.1	35.2	5.5 ± 0.2	46.2 ± 5.2	131.3 ± 16.7	35.6
2	5′**GGAUGCAUUU**	1.8 ± 0.1	7.4 ± 0.1	8.0 ± 0.1	74.4 ± 2.7	214.2 ± 8.4	46.8	7.9 ± 0.1	67.9 ± 7.4	193.7 ± 23.3	47.3
2	5′**UGAUGCAUUG**	1.8 ± 0.1	7.4 ± 0.1	8.1 ± 0.1	75.4 ± 3.9	216.9 ± 12.3	47.2	7.9 ± 0.3	67.6 ± 10.9	192.7 ± 34.4	47.4
2	5′**GUAUCGAUGU**[f,j]	1.9 ± 0.1	5.8 ± 0.1	7.5 ± 0.1	63.4 ± 4.0	180.2 ± 12.7	46.4	7.7 ± 0.3	64.4 ± 10.4	183.0 ± 32.8	46.9
2	5′***GGUCUAGAUU***	2.1 ± 0.1	7.5 ± 0.1	9.1 ± 0.1	89.0 ± 2.0	257.8 ± 6.2	49.2	8.6 ± 0.1	75.6 ± 2.9	216.0 ± 9.5	49.6
2	5′**GUCGCGGU**[l]	2.2 ± 0.1	5.8 ± 0.1	8.0 ± 0.1	57.8 ± 1.0	160.5 ± 3.3	50.0	7.9 ± 0.1	54.3 ± 3.4	149.6 ± 10.9	50.5
2	5′**GUGAUCGU**	2.4 ± 0.2	3.2 ± 0.1	6.0 ± 0.1	47.1 ± 4.2	132.5 ± 13.7	39.2	6.1 ± 0.3	53.2 ± 9.5	152.0 ± 30.5	39.5
2	5′**UGUCGAUG**	2.6 ± 0.1	4.4 ± 0.1	6.3 ± 0.1	68.8 ± 1.4	201.4 ± 4.5	39.8	6.3 ± 0.1	60.5 ± 2.0	174.7 ± 6.6	40.1
2	5′***UGGAUCUG***	2.6 ± 0.1	4.6 ± 0.1	6.5 ± 0.1	66.1 ± 2.6	192.2 ± 8.3	40.7	6.4 ± 0.2	56.2 ± 4.7	160.4 ± 14.9	41.2
2	5′***UUGUCGACGG***[f]	2.9 ± 0.3	8.9 ± 0.1	12.0 ± 0.2	83.8 ± 3.7	231.4 ± 11.0	62.3	11.2 ± 0.1	71.9 ± 1.1	195.7 ± 3.7	62.7
2	5′**GGCAUGUU**[f,k,j]	3.0 ± 0.1	4.9 ± 0.1	6.7 ± 0.1	69.1 ± 2.4	201.0 ± 7.7	41.7	6.7 ± 0.1	65.4 ± 3.9	189.1 ± 12.5	42.0
2	5′**UGCUAGUG**	3.2 ± 0.1	5.1 ± 0.2	7.4 ± 0.1	74.9 ± 1.8	217.7 ± 5.9	44.2	7.2 ± 0.1	64.5 ± 2.6	184.5 ± 8.7	44.7
2	5′***UGCCGGUG***[f,j]	3.8 ± 0.2	8.5 ± 0.1	11.9 ± 0.2	81.6 ± 2.7	216.8 ± 6.8	59.1	11.0 ± 0.2	69.4 ± 0.8	188.1 ± 2.4	62.9
	5′**GUCGGUG**	2.7 ± 0.1	0.0 ± 0.1	3.3 ± 0.1	61.9 ± 2.1	188.9 ± 7.1	25.4	3.5 ± 0.2	56.9 ± 2.7	172.0 ± 9.1	25.7
3	5′**GGUCGCGGUU**[f]	2.6 ± 0.1	5.8 ± 0.1	8.8 ± 0.1	66.5 ± 1.3	186.0 ± 4.1	52.5	8.6 ± 0.1	59.4 ± 1.9	164.0 ± 6.1	52.9
3	5′**GUGAUGCAUUGU**[n]	2.6 ± 0.2	7.0 ± 0.1	9.7 ± 0.2	93.7 ± 4.5	270.9 ± 14.0	50.9	9.2 ± 0.2	79.3 ± 6.1	225.9 ± 19.1	51.4
3	5′**UGUGGCCGUG**	2.7 ± 0.6	7.4 ± 0.1	10.9 ± 0.6	66.2 ± 6.8	178.3 ± 20.2	63.4	10.6 ± 0.7	62.0 ± 7.2	165.6 ± 21.3	64.0
3	5′**UGUCGGUG**[f]	2.8 ± 0.3	0.0 ± 0.1	3.5 ± 0.2	57.3 ± 3.4	173.5 ± 11.4	25.5	3.7 ± 0.3	53.4 ± 5.5	159.3 ± 18.7	26.1
3	5′***UUGGCGCUGG***	3.1 ± 0.2	8.0 ± 0.1	10.8 ± 0.2	76.9 ± 3.0	213.1 ± 9.1	59.2	10.1 ± 0.2	65.3 ± 1.4	177.8 ± 4.3	59.6
3	5′**UUGGCUGG**	3.2 ± 0.2	2.2 ± 0.2	5.2 ± 0.1	49.1 ± 1.5	141.7 ± 5.0	34.0	5.3 ± 0.2	45.9 ± 4.6	130.9 ± 15.2	34.7
3	5′**GGUGGCCGUU**	3.3 ± 0.6	7.3 ± 0.1	11.0 ± 0.6	66.4 ± 6.9	178.6 ± 20.7	64.2	10.5 ± 0.5	57.4 ± 6.5	151.5 ± 19.3	65.1
3	5′**UUGCUAGUGG**	3.4 ± 0.1	5.1 ± 0.1	7.9 ± 0.1	71.9 ± 3.3	206.5 ± 10.5	46.7	7.7 ± 0.1	64.7 ± 3.6	183.8 ± 11.4	47.1
3	5′**GUGGCUGU**[f,n]	3.6 ± 0.1	2.2 ± 0.1	6.0 ± 0.1	52.3 ± 1.2	149.1 ± 6.2	39.2	6.1 ± 0.1	50.4 ± 5.4	142.9 ± 17.5	39.5
3	5′**GUGCUAGUGU**[n]	3.7 ± 0.1	5.1 ± 0.1	8.4 ± 0.1	74.0 ± 2.6	211.3 ± 8.1	48.9	8.2 ± 0.1	66.8 ± 4.2	189.0 ± 13.3	49.3
4	5′**UUGUCGGUGG**[f]	2.7 ± 0.2	0.0 ± 0.2	3.3 ± 0.2	64.0 ± 3.6	195.6 ± 12.3	25.8	3.6 ± 0.2	57.4 ± 1.8	173.2 ± 6.3	26.3
4	5′**GUGUCGGUGU**[f]	3.1 ± 0.1	0.0 ± 0.1	4.0 ± 0.1	65.3 ± 2.3	197.5 ± 7.7	29.3	4.2 ± 0.2	59.6 ± 3.3	178.6 ± 11.1	29.6
4	5′**UGUGGCUGUG**[f,n]	3.5 ± 0.2	2.2 ± 0.1	6.0 ± 0.1	55.5 ± 4.0	159.8 ± 13.1	38.5	6.0 ± 0.2	50.3 ± 3.8	142.7 ± 12.1	39.2
4	5′***GGUGGCUGUU***[f,n]	3.6 ± 0.2	2.2 ± 0.2	6.1 ± 0.1	59.6 ± 1.4	172.5 ± 4.6	39.0	6.1 ± 0.1	50.3 ± 2.2	142.6 ± 7.4	39.7
	5′**AUCGAUA**[m]	4.1 ± 0.1	5.2 ± 0.04	6.1 ± 0.1	56.6 ± 2.0	162.8 ± 6.3	39.4	6.2 ± 0.1	54.2 ± 3.8	154.9 ± 12.4	39.9
	5′**UAUCGAUA**[m]	4.6 ± 0.1	6.5 ± 0.03	7.1 ± 0.1	61.8 ± 3.0	176.2 ± 9.7	44.4	7.2 ± 0.2	61.8 ± 4.9	176.3 ± 15.6	44.6
	5′**UUAUCGAUAA**[m]	5.7 ± 0.1	8.4 ± 0.03	9.2 ± 0.1	82.3 ± 3.7	235.8 ± 11.4	50.8	8.9 ± 0.1	72.6 ± 2.7	205.5 ± 8.8	51.2

[a]Sequences are ordered first by type of terminal base pair, terminal motif, and then in increasing thermodynamic stability. RNA sequences were melted in 1 M NaCl, 10 mM sodium cacodylate, 0.5 mM Na_2EDTA (pH 7) buffer. Italicized sequences have a 15% difference between the melt curve fits and van't Hoff plots and are borderline two-state. Errors associated with $\Delta H°$, $\Delta S°$, and $\Delta G°$ are ±10, ±10, and ±2%, respectively. [b]Bold letters represent the terminal GU motif or terminal AU base pairs. [c]Free energy values are calculated with values from the plots of T_M^{-1} vs ln(C_T/A) using eq 2. [d]Predicted free energy terms are calculated using the nearest-neighbor model parameters from refs *11* and *24*. According to previous rules, only the first terminal GU pair is predicted to contribute a favorable free energy and included in the prediction. [e]Melting temperatures are listed for a total strand concentration of 1×10^{-4} M. [f]Sequences were analyzed with one-dimensional imino proton NMR. [g]Data from ref *8*. [h]Data from ref *9*. [i]Data from ref *23*. [j]These sequences were also melted in 0.15 M KCl, 10 mM $MgCl_2$, 10 mM sodium cacodylate, 0.1 mM Na_2EDTA (pH 7) melting buffer at 280 nm, and no change in thermodynamic stability was observed. [k]Predicted to occur in the duplex formed by let-7 targeting the RAS 3′ UTR (*25*). [l]Predicted to occur in the duplex formed by let-7 targeting the HMGA 3′ UTR (*26*, *27*). [m]Duplexes were measured at 260 nm, the optimal wavelength for AU pair absorption. [n]The duplex contains the sequence 5′GU/3′UG in the third GU nearest-neighbor position.

Current predictions of miRNA−mRNA interactions underestimate the thermodynamic stability of duplexes containing consecutive terminal GU pairs. Three tandem terminal GU motifs, 5′GUU/3′CGG, 5′GGU/3CUG, and 5′AGU/3′UUG, are predicted to occur in duplexes formed by the microRNA let-7 binding to target sequences in the 3′ untranslated regions (UTR) of the RAS and HMGA mRNA (*25*−*27*), which are genes involved in cancer regulatory pathways. These miRNA−mRNA interactions are underestimated by 0.6, 0.7, and 1.4 kcal/mol, respectively (Table 1, footnotes k and l).

Because GU pairs are known to bind metal ions (*28*−*31*), five duplexes were also measured in buffer containing $MgCl_2$. No change in thermodynamic stability was observed for any of the duplexes. A buffer consisting of 0.15 M KCl and 10 mM $MgCl_2$ is more representative of physiological buffer conditions (*32*). Thus, these measurements will be applicable to predictions of miRNA−mRNA target recognition and specificity under biological conditions.

To measure the contributions of hydrogen bonding and stacking to the stability of terminal GU pairs, a duplex with two GU

Table 2: Measuring the Stacking and Hydrogen Bonding Contributions to Terminal GU and AU Pairs[a]

GU pair	terminal GU pairs	$-\Delta\Delta G°_{37}$[b] (kcal/mol)	terminal AU pairs	$-\Delta\Delta G°_{37}$[b] (kcal/mol)
1 + 3′	5′**U**UGCA**GU**	0.8[c]	5′**U**UGCA**AU**	*1.5*[d]
2	5′**GU**UGCA**GU**	1.6[c]	5′**AU**UGCA**AU**	*2.0*[d]
2	5′**GU**CGCG**GU**	2.2	5′**AU**CGCG**AU**	*3.5*[d]
2 + 3′	5′**GU**CGG**UG**	2.7	5′**AU**CGA**UA**	4.1
3	5′**UGU**CGG**UG**	2.8	5′**UAU**CGA**UA**	4.6
4	5′**UUGU**CGG**UGG**	2.7	5′**UUAU**CGA**UAA**	5.7

[a]RNA sequences were melted in 1 M NaCl, 10 mM sodium cacodylate, 0.5 mM Na_2EDTA (pH 7) buffer. [b]Free energy increments are calculated from plots of T_M^{-1} vs $\ln(C_T/A)$ using eq 2. [c]Values from ref *8*. [d]The free energy is predicted from the INN-HB model (*45*) and thermodynamic stabilities of 3′ dangling ends (*8*). The predicted values are consistent with prior similar measurements on duplexes with slightly different stem duplexes (*46*).

Table 3

(A) Parameters for the First GU Terminal Motif[a,b]

		kcal/mol		kcal/mol	closing pair
5′ purine	5′**GU**3′/3′**CG**5′	−2.3 ± 0.1	5′**GG**3′/3′**CU**5′	−1.5 ± 0.1	GC
	5′**AU**3′/3′**UG**5′	−1.6 ± 0.1	5′**AG**3′/3′**UU**5′	−0.8 ± 0.1	AU
5′ pyrimidine	5′**CU**3′/3′**GG**5′	−1.9 ± 0.1	5′**CG**3′/3′**GU**5′	−1.8 ± 0.1	CG
	5′**UU**3′/3′**AG**5′	−1.1 ± 0.1	5′**UG**3′/3′**AU**5′	−1.0 ± 0.1	UA

(B) Parameters for Additional GU Pairs[c]

second GU terminal pair	−0.7 ± 0.1 kcal/mol
third GU terminal pair	−0.5 ± 0.1 kcal/mol
5′GU/3′UG bonus[d]	−0.4 ± 0.1 kcal/mol

[a]Values are calculated from a multiple linear regression of 38 experimentally measured free energies for two-state terminal motifs measured in 1 M NaCl, 10 mM sodium cacodylate, 0.5 mM Na_2EDTA (pH 7.0) buffer. [b]Seven sequences used in the linear regression analysis are reported in refs *8*, *9*, and *23*. [c]If the sequence has more than three GU terminal pairs, then no additional stability is added. [d]This bonus is added only if the third terminal GU nearest neighbor has this particular sequence.

pairs and a 3′ dangling end was studied (Table 2). The free energy of the tandem terminal GU pair in 5′**GU**CGCG**GU** is −2.2 kcal/mol. Adding a single G nucleotide to the 3′ end, 5′**GU**CG**GUG**, changed the stability of the terminal motif by −0.5 kcal/mol. However, adding a 5′ U nucleotide to create a third GU pair in 5′**UGU**CG**GUG** does not contribute any additional thermodynamic stability and provides no evidence for stabilizing hydrogen bonding. On the other hand, in previous research on consecutive terminal mismatches, the thermodynamic stability of adding a G nucleotide to create a second GU pair, 5′**GU**UGCA**GU**, to a duplex with a single GU pair and a dangling nucleotide, 5′**U**UGCA**GU**, increased the thermodynamic stability by 0.8 kcal/mol (*8*). Furthermore, a fourth GU pair adds no more stability than three GU pairs or two GU pairs with a 3′ G. Thus, the additional stability of a terminal GU pair depends on the distance from the Watson−Crick core helix. In contrast, consecutive terminal AU pairs increase in stability with each additional 3′ and 5′ nucleotide added for up to four consecutive terminal AU pairs, demonstrating the energetic contributions of both hydrogen bonding and stacking (Table 2). GU pairs show a different pattern. Near the last Watson−Crick pair, both stacking and hydrogen bonding apparently contribute to the free energy of the terminal GU motif. However, as the number of terminal GU pairs increases, the stability of each additional GU pair decreases. Duplexes with three terminal GU pairs show less orientation dependence of the last GU pair than in the first pair, and the additional stability may be due largely to stacking. The fourth GU pair adds no further stability, which is consistent with previous observations of consecutive terminal mismatches (*8*) and measurements of RNA persistence length, a measure of the stiffness and flexibility of a polymer (*33*−*35*).

FIGURE 2: Example of a duplex containing the sequence 5′GU/3′UG in the third GU nearest-neighbor position and all possible tandem GU nearest neighbors. The nearest neighbors in the terminal GU motif are as follows: first, 5′CU/3′GG; second, 5′UG/3′GU; third, 5′GU/3′UG; fourth, 5′UU/3′GG. Note that 5′UU/3′GG and 5′GG/3′UU are equivalent nearest neighbors.

The measurements and observations in Tables 1 and 2 lead to new rules for predicting the thermodynamic stabilities of consecutive terminal GU pairs (Table 3). Previous prediction rules considered only a single terminal GU mismatch and no additional terminal GU pairs. A second and third GU pair add −0.7 and −0.5 kcal/mol, respectively. The 5′GU/3′UG motif is especially stable as the third nearest-neighbor pair (Figure 2); 38 measurements for terminal GU pairs were fit with a linear regression analysis. The r^2 value for the fit was 0.98. The spreadsheet and statistics for the linear regression are presented as Supporting Information.

The parameters for the first GU pair show the most dependence on stacking on the Watson−Crick pair and the orientation of the GU pair. A GU pair stacked on a GC or CG pair is more favorable than one stacked on an AU or UA pair, respectively. If

the 5′ nucleotide in the Watson−Crick pair is a purine, different orientations of the adjacent GU pair show very different stabilities, and the UG pair is more stable than the GU pair. For example, 5′GU/3′CG and 5′GG/3′CU sequences have stabilities of −2.3 and −1.5 kcal/mol, respectively. If the 5′ nucleotide in the Watson−Crick pair is a pyrimidine, then either orientation of the GU pair has the same stability. These observations are consistent with ultrafast fluorescence spectroscopy studies of the interplay between stacking and hydrogen bonding in terminal purine-U pairs (*36*). 5′CG/3′GU and 5′CU/3′GG sequences have stabilities of −1.8 and −1.9 kcal/mol, respectively, and 5′UG/3′AU and 5′UU/3′AG sequences have stabilities of −1.0 and −1.1 kcal/mol, respectively. These parameter pairs are not combined to maintain consistency with a physical model that considers energetic contributions of stacking effects.

To test whether consecutive GU pairs could form a stable helix in the absence of a central core with Watson−Crick pairs, a helix composed solely of GU pairs, $(5'GUGUUGGUGUG)_2$, was designed. The melting behavior of this duplex was observed at 260, 280, and 300 nm, and no clear transition was observed at 260 or 280 nm. A transition from high to low absorbance at 300 nm was observed at 23.88 °C at 1.54×10^{-4} M RNA. This type of transition, a decrease in hyperchromicity at 300 nm, has been observed for terminal Hoogsteen pairs in terminal mismatches (*37*). Thus, an all-GU pair helix may form but have very different base stacking and dipole interactions. The normalized data provide an estimate of the thermodynamic stability: −60.3 kcal/mol enthalpy, −185.7 cal K^{-1} mol^{-1} entropy, and −2.7 kcal/mol free energy at 1.54×10^{-4} M RNA. A similar helix of only AU pairs, $(5'AUAUUAAUAUA)_2$, showed a transition at 260 nm and no measurable change in absorbance at 300 nm. The estimated thermodynamic stability of this all-AU duplex is as follows: −74.5 kcal/mol enthalpy, −221.0 cal K^{-1} mol^{-1} entropy, and −6.0 kcal/mol free energy at 9.42×10^{-5} M RNA.

Figure 3 shows imino proton spectra of helices with two, three, or four terminal GU pairs. One-dimensional proton NMR can reveal imino protons that are protected from exchange with water by hydrogen bonds and thus provide evidence of hydrogen bonding within the terminal GU pairs. The terminal pair in a helix is more flexible, and the imino protons therefore exchange more rapidly with water and are usually not observed in proton NMR even for terminal Watson−Crick pairs (*15*, *38*). The imino protons in GC Watson−Crick and GU pairs typically resonate between 12 and 13.5 ppm and between 10 and 13 ppm, respectively. The number and chemical shifts of the peaks in the imino proton spectra are consistent with a single duplex conformation. The number, sharpness, and chemical shifts of the imino proton peaks show a strong sequence dependence in different GU terminal motifs. The upfield peaks are sometimes weak and broad but are indicative of hydrogen-bonded GU pairs. In contrast, imino proton spectra of duplexes with two or three consecutive UU pairs showed no imino proton resonances for the U nucleotides (*8*). Surprisingly, some terminal GU motifs exhibit an odd number of peaks (Figure 3c,d,h−j,m,n), which suggests that different kinds of GU pairs may form. Figure 1 shows just four examples of the many different ways GU pairs can form hydrogen bonds. In several cases, there is an even number of imino protons that can be assigned to the terminal GU pairs, but the intensity and width of the peaks are not the same, which suggests different dynamics for the nucleotides that may transiently form pairs or different GU pair conformations with a single hydrogen bond. The imino proton spectra show that the conformations and dynamics of the G and U nucleotides in terminal motifs are sequence- and context-dependent.

DISCUSSION

Accurate Thermodynamic Parameters for GU Pairs Are Important for Predictions of MicroRNAs and Design of Therapeutic RNA Oligomers. The thermodynamic stability of the duplex formed by a miRNA and mRNA target sequence is one factor in determining the specificity and mechanism of RNA interference (*3*−*5*). Duplexes with perfect matches and favorable stability follow a cleavage mechanism, and duplexes with many mismatches and intermediate stability follow a translation inhibition mechanism (*3*). Duplexes containing GU mismatches are the exception to this general trend (*4*). This may be the result of incomplete rules for predicting the thermodynamic stabilities of duplexes with GU pairs and the idiosyncratic, non-nearest-neighbor effects observed for GU pairs (*9*, *11*−*16*, *39*). Some prediction programs restrict the allowed number of GU pairs (*40*). This work demonstrates that previous prediction rules underestimated the thermodynamic stabilities for duplexes with consecutive terminal GU pairs by an average of 0.5, 1.9, 3.2, and 3.7 kcal/mol for single, tandem, triple, and quadruple terminal GU pairs, respectively (Table 1, comparison of predicted and experimental duplex free energies). The new rules for predicting helices with terminal GU pairs (Table 3) will be incorporated into RNA secondary structure prediction programs, such as RNAStructure, Vienna Package, mfold/unafold, and Sfold (*41*−*44*), and will contribute to improving the prediction of mRNA target structures and miRNA−mRNA interactions.

The Thermodynamic Stability Contributions of GU Pairs Depend on the Position of the GU Pair in the Helix. Previous studies of tandem GU pairs focused on GU pairs in the middle of a helix (*11*−*14*). Tandem GU pairs in the middle of a helix are thermodynamically unstable and have positive nearest-neighbor free energy values (*11*, *24*). The one exception, 5′GGUC/3′CUGG, has a favorable free energy for a tandem internal GU pair only in this particular sequence of surrounding Watson−Crick pairs, which is a non-nearest-neighbor effect. In contrast, all the tandem terminal GU pairs are thermodynamically favorable. At the end of a helix, GU pairs may have the flexibility to adopt a conformation that maximizes hydrogen bonding and stacking interactions but is not accommodated into an A-form RNA helix in an energetically favorable way. Thus, the unfavorable stabilities of internal GU pairs may reflect an energetically unfavorable disruption of the A-form helix.

Different Orientations of Terminal GU Pairs Have Different Conformations with Equivalent Thermodynamic Stabilities. The thermodynamic measurements and new prediction rules show a dependence on the 5′/3′ orientation of the GU pair only in the cases of a single terminal GU pair and when the third nearest-neighbor pair has the sequence 5′GU/3′UG (Table 3). The additional stability for a second and third GU pair has no significant dependence on the orientation of the GU pair in most cases. However, the imino proton spectra show a different number of peaks and different chemical shifts for sequences with different orientations of terminal GU pairs (Figure 3). This suggests that different orientations of the GU pair may adopt different conformations, but that these different conformations have equivalent thermodynamic stabilities.

For example, in tandem terminal GU pairs, comparison of $(5'\mathbf{UU}GUCGAC\mathbf{GG})_2$ and $(5'\mathbf{UU}AUCGAU\mathbf{GG})_2$ (Figure 3c,d)

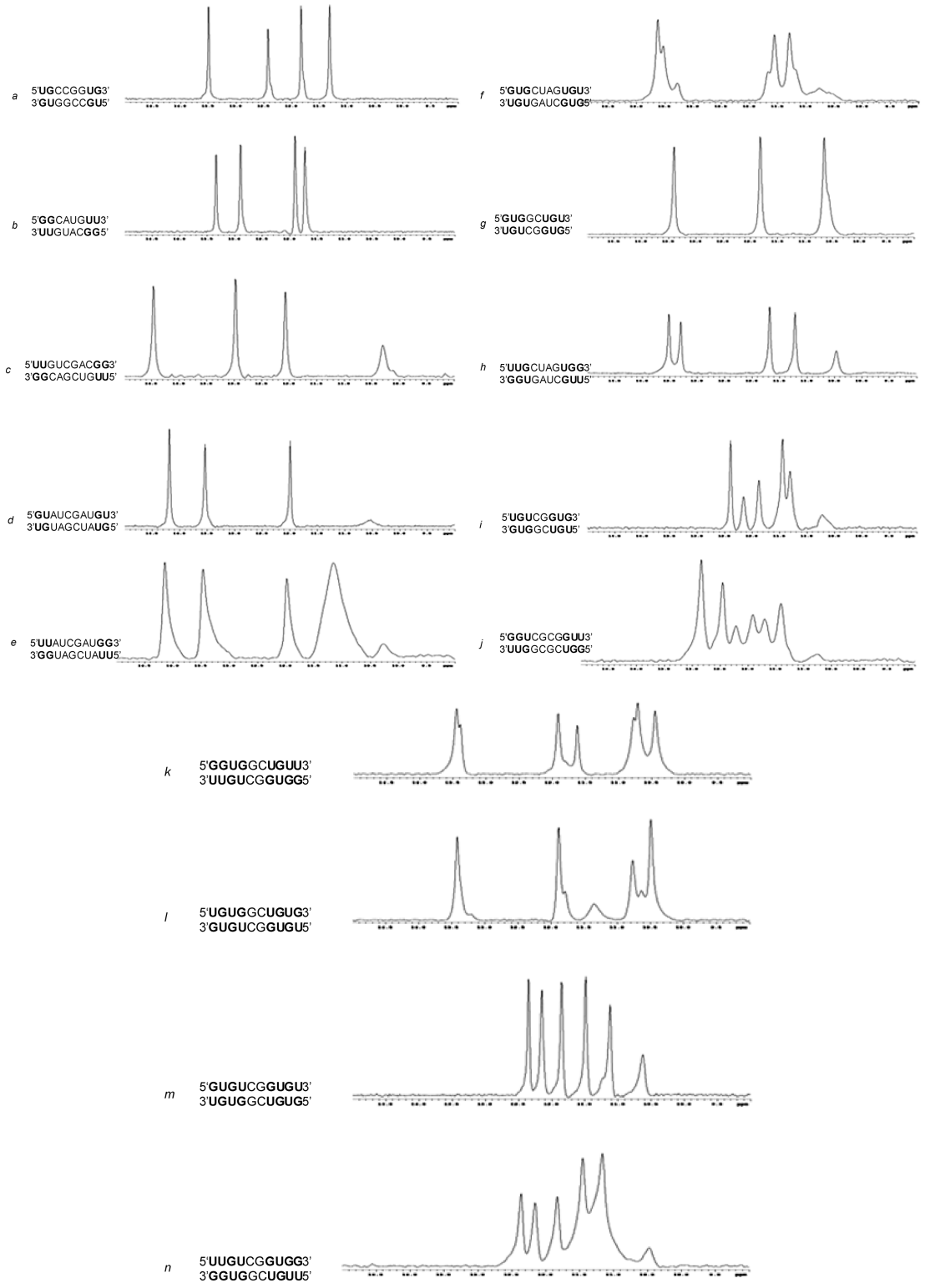

FIGURE 3: One-dimensional imino proton spectra at 1 °C in 10 mM NaCl, 10 mM NaH_2PO_4, 0.5 mM Na_2EDTA (pH 6.0) buffer. Chemical shifts are referenced to the position of the water peak, which has measured chemical shifts relative to trimethylsilyl propionate in this NMR buffer. The 2 × 2 terminal GU duplexes: (a) 5′**UGCCGGUG**, (b) 5′**GGCAUGUU**, (c) 5′**UUGUCGACGG**, (d) 5′**GUAUCGAUGU**, and (e) 5′**UUAUCGAUGG**. The 3 × 3 GU duplexes: (f) 5′**GUGCUAGUGU** at 10 °C, (g) 5′**GUGGCUGU**, (h) 5′**UUGCUAGUGG**, (i) 5′**UGUCGGUG**, and (j) 5′**GGUCGCGGGU**. The 4 × 4 GU duplexes: (k) 5′**GGUGGCUGUU**, (l) 5′**UGUGGCUGUG**, (m) 5′**GUGUCGGUGU**, and (n) 5′**UUGUCGGUGG**.

shows that changing the closing Watson−Crick pair from a CG pair to a UA pair changes the number of imino protons protected from exchange with water. The (5′**UU**AUCGAU**GG**)$_2$ helix has an additional broad peak, which suggests that stacking on the last Watson−Crick pair can affect the conformation of the terminal GU pairs. Comparison of (5′**UU**AUCGAU**GG**)$_2$ with (5′**GU**AUCGAU**GU**)$_2$ (Figure 3d,e) shows that the orientation of the last GU pair also changes the number of peaks in the spectrum. (5′**GU**AUCGAU**GU**)$_2$ has no large broad peak near 11 ppm, but only one small peak at 10.5 ppm. Although the imino proton

spectra for (5′**UU**AUCGAU**GG**)$_2$ and (5′**GU**AUCGAU**GU**)$_2$ are distinctly different, the thermodynamic stability for both terminal GU motifs is similar.

Although the fourth GU pair adds no additional thermodynamic stability, the addition of a fourth GU pair does change the number, sharpness, and chemical shifts of imino protons in the terminal GU pair motifs. There are two cases in which a triple GU pair and both orientations of the fourth GU pair can be compared. Duplex (5′**GUGGCUGU**)$_2$ (Figure 3g) shows three imino protons, one proton resonance for the core GC pair, and two proton resonances for a GU pair. After the addition of a fourth GU pair, several more imino protons are observed. Duplex (5′**GGUGGCUGUU**)$_2$ (Figure 3h) has seven imino protons similar in sharpness and intensity, which accounts for the core GC pair and three GU pairs. Duplex (5′**UGUGGCUGUG**)$_2$ (Figure 3l) has a fourth GU pair in the other orientation and shows four strong, sharp peaks and three or four less intense, broad peaks. The free energies for these three terminal GU motifs (5′CUGU, 5′CUGUU, and 5′CUGUG) all have similar thermodynamic stabilities of −3.6, −3.6, and −3.5 kcal/mol, respectively, which are within experimental error (Table 1). Similarly, (5′**UGUCGGUG**)$_2$ (Figure 3i) shows six imino proton resonances with varying sharpness and intensities. One imino proton resonance can be attributed to the core CG pair and five resonances to the three terminal GU pairs. When a fourth GU pair is added, many of the resonances become sharper. The spectrum for (5′**GUGU**CG**GUGU**)$_2$ (Figure 3m) shows five very sharp intense resonances and only one small broad resonance. The imino proton resonances for (5′**UUGU**CG**GUGG**)$_2$ (Figure 3n) in which the fourth GU pair has a different orientation have broad overlapping bases and are less distinct. The relative intensities of the peaks also change; a group of two resonances and a group of three resonances have similar relative intensities, while one resonance remains very weak and broad. Thus, different stacking orientations for the terminal GU pair may induce different hydrogen bonding conformations or differently protect imino protons from exchange with water.

Base Stacking Affects the Thermodynamic Stability and Conformation throughout the Helix and in the Special Case of the 5′GU/3′UG Bonus. Three pairs of duplexes have the same sequence but in the reverse 5′ to 3′ orientation. These duplexes have different thermodynamic stabilities and imino proton spectra, which suggests that stacking plays an important role in the stability and structure of terminal GU motifs. For example, (5′**GUGGCUGU**)$_2$ and (5′**UGUCGGUG**)$_2$ have terminal GU stabilities of −3.6 and −2.8 kcal/mol, respectively (Table 1). (5′**GUGGCUGU**)$_2$ shows three sharp imino proton resonances spread over a 3 ppm chemical shift range, and (5′**UGUCGGUG**)$_2$ shows two strong, sharp resonances, three less intense resonances, and one weak broad resonance within the 2 ppm chemical shift range (Figure 3g,i). (5′**GGUGGCUGUU**)$_2$ has a terminal GU thermodynamic stability of −3.6 kcal/mol and shows eight sharp imino proton peaks over a 3 ppm chemical shift range. In contrast, (5′**UUGUCGGUGG**)$_2$ has the same sequence in the opposite 5′ to 3′ orientation but has a terminal GU thermodynamic stability of −2.7 kcal/mol and shows six broad imino proton resonances over a 2 ppm chemical shift range (Table 1 and Figure 3k,n). Similarly, when (5′**UGUGGCUGUG**)$_2$ and (5′**UUGUCGGUGG**)$_2$ are compared, the terminal GU thermodynamic stabilities are −3.1 and −2.7 kcal/mol (Table 1), respectively, and they show three strong, sharp peaks with three weaker peaks over a 3 ppm range versus six sharp peaks over a 2 ppm range (Figure 3l,m). The most stable duplexes in each of these three cases, (5′**GUGGCUGU**)$_2$, (5′**GGUGGCUGUU**)$_2$, and (5′**UGUGGCUGUG**)$_2$, all share in common the first GU pair stacking on a CG, i.e., 5′CU/3′GG; the 5′GU/3′UG sequence in the third GU nearest-neighbor position; and an imino proton chemical shift dispersion of 3 ppm.

The effects of stacking and the positional dependence of the stabilities of GU pairs are apparent in the bonus for the 5′GU/3′UG sequence in the third nearest-neighbor position (Figure 2). The bonus of −0.4 kcal/mol for the 5′GU/3′UG sequence is statistically significant (Table 3B and Table 2 of the Supporting Information) and supported by the imino proton NMR spectra (Figure 3). The additional stability of the 5′GU/3′UG bonus is most clearly demonstrated in the comparison of the terminal GU thermodynamic stabilities of (5′**GUGCUAGUGU**)$_2$ versus (5′**UUGCUAGUGG**)$_2$ and (5′**GUGGCUGU**)$_2$ versus (5′**UUGGCUGG**)$_2$, which are identical except for the nearest-neighbor pair in the third position (Table 1). The 0.4 kcal/mol difference in each of the terminal GU motifs in the self-complementary duplexes cannot be explained by other terminal stacking effects or Watson−Crick stem effects in these two cases. The 5′GU/3′UG sequence is also exceptionally stable in internal GU pairs in the particular sequence context of 5′GGUC/3′CUGG and has an unfavorable free energy in all other internal pairs (*24*). Thus, favorable stabilities for the 5′GU/3′UG sequence may result from stacking interactions extending through the helix and beyond the immediate nearest neighbors.

CONCLUSIONS

The thermodynamic stabilities of terminal GU pairs are favorable and add stability up to three GU pairs extending from a Watson−Crick stem helix. The 5′GU/3′UG sequence is especially stable in the third GU nearest-neighbor position. Imino proton NMR spectra confirm the formation of hydrogen-bonded GU pairs and suggest that terminal GU pair motifs may have very different conformations even if the thermodynamic stabilities are similar. The new rules for predicting the thermodynamics stabilities of terminal GU pairs will contribute to the improvement of RNA structure prediction programs and identification of small RNA−mRNA interactions.

ACKNOWLEDGMENT

We thank Steven Harris for assistance in the collection of imino proton NMR spectra and Koree Clanton-Arrowood and Dr. Xiaobo Gu for advice and assistance with optical melting experiments and analysis of oligomer purity.

SUPPORTING INFORMATION AVAILABLE

Linear regression analysis and statistics. This material is available free of charge via the Internet at http://pubs.acs.org.

REFERENCES

1. Castanotto, D., and Rossi, J. J. (2009) The promises and pitfalls of RNA-interference-based therapeutics. *Nature 457*, 426–433.
2. Carthew, R. W., and Sontheimer, E. J. (2009) Origins and Mechanisms of miRNAs and siRNAs. *Cell 136*, 642–655.
3. Haley, B., and Zamore, P. D. (2004) Kinetic Analysis of the RNAi Enzyme Complex. *Nat. Struct. Biol. 11*, 599–606.
4. Doench, J. G., and Sharp, P. A. (2004) Specificity of microRNA Target Selection in Translational Repression. *Genes Dev. 18*, 504–511.
5. Ameres, S. L., Martinez, J., and Schroeder, R. (2007) Molecular Basis for Target RNA Recognition and Cleavage by Human RISC. *Cell 130*, 101–112.

6. Ding, Y., and Lawrence, C. E. (2001) Statistical Prediction of Single-Stranded Regions in RNA Secondary Structure and Application to Predicting Effective Antisense Target Sites and Beyond. *Nucleic Acids Res. 29*, 1034–1046.
7. Tafer, H., Ameres, S. L., Obernosterer, G., Gebeshuber, C. A., Schroeder, R., Martinez, J., and Hofacker, I. L. (2008) The impact of target accessibility on the design of effective siRNAs. *Nat. Biotechnol. 26*, 578–583.
8. Clanton-Arrowood, K., McGurk, J., and Schroeder, S. J. (2008) 3′ Terminal Nucleotides Determine Thermodynamic Stabilities of Mismatches at the Ends of RNA Helices. *Biochemistry 47*, 13418–13427.
9. Freier, S. M., Kierzek, R., Caruthers, M. H., Neilson, T., and Turner, D. H. (1986) Free energy of GU contributions and other terminal mismatches to helix stability. *Biochemistry 25*, 3209–3213.
10. Sugimoto, N., Kierkek, R., Freier, S. M., and Turner, D. H. (1986) Energetics of Internal GU Mismatches in Ribonucleotide Helixes. *Biochemistry 25*, 5755–5759.
11. He, L., Kierzek, R., SantaLucia, J., Jr., Walter, A. E., and Turner, D. H. (1991) Nearest-neighbor parameters for GU mismatches. *Biochemistry 30*, 11124–11132.
12. McDowell, J. A., and Turner, D. H. (1996) Investigation of the structural basis for thermodynamic stabilities of tandem GU mismatches: solution structure of $(rGAGGUCUC)_2$ by two-dimensional NMR and simulated annealing. *Biochemistry 35*, 14077–14089.
13. McDowell, J. A., He, L., Chen, X., and Turner, D. H. (1997) Investigation of the structural basis for thermodynamic stabilities of tandem GU wobble pairs: NMR structures of $(rGGAGUUCC)_2$ and $(rGGAUGUCC)_2$. *Biochemistry 36*, 8030–8038.
14. Chen, X., McDowell, J. A., Kierzek, R., Krugh, T. R., and Turner, D. H. (2000) Nuclear magnetic resonance spectroscopy and molecular modeling reveal that different hydrogen bonding patterns are possible for GU pairs: One hydrogen bond for each GU pair in $r(GGCGUGCC)_2$ and two for each GU pair in $r(GAGUGCUC)_2$. *Biochemistry 39*, 8970–8982.
15. Schroeder, S. J., and Turner, D. H. (2001) Thermodynamic stabilities of internal loops with GU closing pairs in RNA. *Biochemistry 40*, 11509–11517.
16. Tolbert, B. S., Kennedy, S. D., Schroeder, S. J., Krugh, T. R., and Turner, D. H. (2007) NMR structures of $(rGCUGAGGCU)_2$ and $(rGCGGAUGCU)_2$: Probing the structural features that shape the thermodynamic stability of GA pairs. *Biochemistry 46*, 1511–1522.
17. Schroeder, S. J., Fountain, M. A., Kennedy, S. D., Lukavsky, P. J., Puglisi, J. D., Krugh, T. R., and Turner, D. H. (2003) Thermodynamic Stability and Structural Feautures of the J4/5 Loops in a *Pneumocystis carini* Group I Intron. *Biochemistry 42*, 14184–14196.
18. Stombaugh, J., Zirbel, C. L., and Leontis, N. B. (2009) Frequency and Isostericity of RNA Base Pairs. *Nucleic Acids Res. 37*, 2294–2312.
19. Petersheim, M., and Turner, D. H. (1983) Base-stacking and base-pairing contributions to helix stability: Thermodynamics of double-helix formation with CCGG, CCGGp, CCGGAp, ACCGGp, CCGGUp, and ACCGGUp. *Biochemistry 22*, 256–263.
20. Borer, P. N., Dengler, B., Tinoco, I., Jr., and Uhlenbeck, O. C. (1974) Stability of ribonucleic double-stranded helices. *J. Mol. Biol. 86*, 843–853.
21. Freier, S. M., Kierzek, R., Jaeger, J. A., Sugimoto, N., Caruthers, M. H., Neilson, T., and Turner, D. H. (1986) Improved free-energy parameters for predictions of RNA duplex stability. *Proc. Natl. Acad. Sci. U.S.A. 83*, 9373–9377.
22. Lukavsky, P., and Puglisi, J. (2001) RNAPack: An integrated NMR approach to RNA structure determination. *Methods 25*, 316–332.
23. Sugimoto, N., Kierkek, R., and Turner, D. H. (1987) Sequence Dependence for the Energetics of Terminal Mismatches in Ribooligonucleotides. *Biochemistry 26*, 4559–4562.
24. Turner, D. H. (2000) Conformational Changes. In Nucleic Acids: Structures, Properties, and Functions (Bloomfield, V. A., Crothers, D. M., and Tinoco, I., Jr., Eds.) pp 259−334, University Science Books, Sausalito, CA.
25. Johnson, S. M., Grosshans, H., Shingara, J., Byrom, M., Jarvis, R., Cheng, A., Labourier, E., Reinert, K. L., Brown, D., and Slack, F. J. (2005) RAS is regulated by the let-7 microRNA family. *Cell 120*, 635–647.
26. Mayr, C., Hemann, M. T., and Bartel, D. P. (2007) Disrupting the pairing bewteen let-7 and Hmga2 enhances oncogenic transformation. *Science 315*, 1576–1579.
27. Shell, S., Park, S.-M., Radjabi, A. R., Schickel, R., Kistner, E. O., Jewell, D. A., Feig, C., Lengyel, E., and Peter, M. E. (2007) Let-7 expression defines two different stages of cancer. *Proc. Natl. Acad. Sci. U.S.A. 104*, 11400–11405.
28. Serra, M., Baird, J., Dale, T., Fey, B., Retatagos, K., and Westhof, E. (2002) Effects of magnesium ions on the stabilization of RNA oligomers of defined structures. *RNA 8*, 307–323.
29. Gonzalez, R. L., Jr., and Tinoco, I., Jr. (1999) Solution structure and thermodynamics of a divalent metal ion binding site in an RNA pseudoknot. *J. Mol. Biol. 289*, 1267–1282.
30. Keel, A., Rambo, R., Batey, R., and Kieft, J. (2007) A general strategy to solve the phase problem in RNA crystallography. *Structure 15*, 761–772.
31. Wang, W., Zhao, J., Han, Q., Wang, G., Yang, G., Shallop, A. J., Liu, J., Gaffney, B. L., and Jones, R. A. (2009) Modulation of RNA Metal Binding by Flanking Bases: ^{15}N NMR Evaluation of GC, Tandem GU, and Tandem GA Sites. *Nucleosides, Nucleotides Nucleic Acids 28*, 424–434.
32. Williams, A., Longfellow, C., Freier, S., Kierzek, R., and Turner, D. (1989) Laser temperature-jump, spectroscopic, and thermodynamic study of salt effects on duplex formation by dGCATGC. *Biochemistry 28*, 4283–4291.
33. Seol, Y., Skinner, G. M., and Visscher, K. (2004) Elastic properties of single-stranded charged homopolymeric ribonucleotide. *Phys. Rev. Lett. 10*, 118102.
34. Seol, Y., Skinner, G. M., and Visscher, K. (2007) Stretching of homopolymeric RNA reveals single-stranded helices and base-stacking. *Phys. Rev. Lett. 98*, 158103–158107.
35. Hyeon, C., Dima, R. I., and Thirumalai, D. (2006) Size, shape, and flexibility of RNA Structures. *J. Chem. Phys. 125*, 194905–194915.
36. Liu, J. D., Zhoa, L., and Xia, T. (2008) The dynamic structural basis of differential enhancement of conformational stability by 5′ and 3′ dangling ends in RNA. *Biochemistry 47*, 5962–5975.
37. Miyoshi, D., Nakamura, K., Tateishi-Karimata, H., Ohmichi, T., and Sugimoto, N. (2009) Hydration of Watson-Crick base pairs and dehydration of Hoogsteen base pairs inducing structural polymorphism under molecular crowding conditions. *J. Am. Chem. Soc. 131*, 3522–3531.
38. Schroeder, S. J., and Turner, D. H. (2000) Factors affecting the thermodynamic stability of small asymmetric internal loops in RNA. *Biochemistry 39*, 9257–9274.
39. Walter, A. E., Wu, M., and Turner, D. H. (1994) The stability and structure of tandem GA mismatches in RNA depend on closing base pairs. *Biochemistry 33*, 11349–11354.
40. Ragan, C., Cloonan, N., Grimmond, S. M., Zuker, M., and Ragan, M. A. (2009) Transcriptome-wide prediction of miRNA targets in human and mouse using FASTH. *PLoS One 4*, e5745.
41. Mathews, D. H., Disney, M. D., Childs, J. L., Schroeder, S. J., Zuker, M., and Turner, D. H. (2004) Incorporating chemical modification constraints into a dynamic programming algorithm for prediction of RNA secondary structure. *Proc. Natl. Acad. Sci. U.S.A. 101*, 7287–7292.
42. Gruber, A., Lorenz, R., Bernhart, S., Neubock, R., and Hofacker, I. (2008) The Vienna RNA Websuite. *Nucleic Acids Res. 36*, W70–W74.
43. Zuker, M. (2003) Mfold Web Server for Nucleic Acid Folding and Hybridization Prediction. *Nucleic Acids Res. 31*, 3406–3415.
44. Ding, Y., Chan, C. Y., and Lawrence, C. E. (2004) Sfold Web Server for Statistical Folding and Rational Design of Nucleic Acids. *Nucleic Acids Res. 32*, W135–W141.
45. Xia, T., Santa Lucia, J., Jr., Burkard, M. E., Kierzek, R., Schroeder, S. J., Jiao, X., Cox, C., and Turner, D. H. (1998) Thermodynamic Parameters for an Expanded Nearest-neighbor Model for Formation of RNA Duplexes with Watson-Crick Base Pairs. *Biochemistry 37*, 14719–14735.
46. Sugimoto, N., Kierzek, R., and Turner, D. H. (1987) Sequence Dependence for the Energetics of Dangling Ends and Terminal Base Pairs in Ribonucleic Acid. *Biochemistry 26*, 4554–4558.